Biomaterials Science

ROYAL SOCIETY OF CHEMISTRY

PAPER

View Article Online
View Journal | View Issue

Cite this: *Biomater. Sci.*, 2023, **11**, 678

Baicalein-functionalized collagen scaffolds direct neuronal differentiation toward enhancing spinal cord injury repair†

Lin Qian,‡[a] Keni Yang,‡[a] Xiru Liu,[a] Lulu Zhang,[a] Haitao Zhao,[a] Lin-Zi Qiu,[a] Yun Chu,[a] Wangping Hao,[a] Yan Zhuang,[a] Yanyan Chen*[a] and Jianwu Dai *[a,b]

Spinal cord injury (SCI) repair remains a major challenge in clinics. Though neural stem cells (NSCs) have shown great potentials in SCI treatment, their applications were hampered since they primarily differentiate into astrocytes rather than neurons in the injured area, indicating a high demand for effective strategies to direct neuronal differentiation. Baicalein is a clinical drug with multiple pharmacological activities, while its effects on NSCs have rarely been reported. In the current work, inspired by a similarity of the metabolic reprogramming required in neuronal differentiation and that involved in chemoresistance reversal of cancer cells induced by baicalein, we studied the role of baicalein in NSC differentiation and discovered its promotion effects on neuronal differentiation. Based on this observation, baicalein-functionalized collagen scaffolds (BFCSs) were developed and applied for SCI treatment. The BFCSs released the payload in a sustained way and possessed comparable physical properties to the commonly used collagen. Both *in vitro* studies with primary NSCs and *in vivo* studies in SCI rats showed that the BFCSs containing a low amount of baicalein can facilitate not only neurogenesis and axon extension, but also reduce astrocyte production and glial scar formation. More importantly, the BFCS implantation led to improvement in the motor functional recovery of SCI rats. Thus, the BFCSs provided a potential strategy to induce neuronal differentiation towards facilitating SCI repair, as well as for the treatment of other central nervous system injuries.

Received 9th September 2022,
Accepted 5th December 2022

DOI: 10.1039/d2bm01467j

rsc.li/biomaterials-science

Introduction

Spinal cord injury (SCI) is one of the most devastating diseases, which disrupts the neural networks in spinal cord tissue and usually leads to a permanent functional impairment below the level of injury in patients.[1,2] Unfortunately, to date, there has been no effective therapy for SCI in clinics. This is mainly because neurons, the basic unit of the nervous system, lack a capacity to self-renew and compensate for the lost neuronal cells during SCI.[3] In addition, an inhibitory microenvironment after injury is formed with a series of pathological reactions, including – for instance – inflammation burst, neurotoxin release, hypoxia and edema, aggravating nerve cell damage and tissue injury.[1,4,5]

In recent years, neural stem cells (NSCs) have attracted increasing attention in SCI repair, due to their potential to differentiate into neural cells and subsequently reconstruct nerve networks with the host circuitry.[6,7] Besides, a beneficial effect of the paracrine vesicles and molecules from NSCs in immune regulation and blood vessel formation in injured tissues has been reported.[8,9] In our previous studies, we have discovered that the endogenous NSCs in spinal cords migrate to the lesion area after activation by acute injury.[10,11] Thus, regulating NSCs *in situ* to facilitate their migration, proliferation and neuronal differentiation can serve as a promising strategy for SCI treatment.[12] Alternatively, several studies have tried to transplant exogeneous NSCs in the lesion sites of SCI animals, which showed improvement effects on SCI recovery to a certain extent.[13,14] Despite the great advantages of NSCs, once arriving around the injured area of spinal cords, they tend to differentiate into astrocytes rather than neurons regardless of their source (endogenous or exogenous ones), mainly due to the existence of the inhibitory microenvironment following SCI.[15–17] The differentiated astrocytes from NSCs can be subsequently involved in the formation of a glial scar at the lesion site, leading to a chemical and physical barrier that further diminishes neural regeneration.[13,18] Though several growth

[a]*Division of Nanobiomedicine, Suzhou Institute of Nano-Tech and Nano-Bionics, Chinese Academy of Sciences, Suzhou, 215123 China.*
E-mail: yychen2006@sinano.ac.cn, jwdai@genetics.ac.cn
[b]*Key Laboratory of Molecular Developmental Biology, Institute of Genetics and Developmental Biology, Chinese Academy of Sciences, Beijing, 100101 China*

†Electronic supplementary information (ESI) available. See DOI: **https://doi.org/10.1039/d2bm01467j**

‡These authors contributed equally.

factors, antibodies or chemical agents have been used to improve the differentiation potential of NSCs into neurons, hardly any of them has so far demonstrated sufficient efficacy in clinical trials.[19] Therefore, strategies directing neural differentiation of NSCs remain highly sought after in the SCI treatment.

Baicalein, a flavone originally isolated from the root of *Scutellaria baicalensis* and *Scutellaria lateriflora*, is a clinical drug with multiple pharmacological activities but low side effects, including anti-cancer, anti-inflammatory and antioxidant effects among others.[20–22] In the treatment of cancer, baicalein has been discovered to reduce aerobic glycolysis of cancer cells by suppressing the expression of hexokinase-2 (HK2), lactate dehydrogenase A (LDHA) and pyruvate dehydrogenase kinase-1 (PDK1), by which the drug resistance of cancer cells to chemotherapy was reversed under hypoxia.[23,24] It is interesting to notice that this metabolic alteration induced by baicalein in cancer cells together with a series of enzymes involved were also reported in the process of neuronal differentiation in NSCs. It has been known that neural stem/progenitor cells reply on a metabolic process called aerobic glycolysis, while neurons use a process named oxidative phosphorylation.[25,26] Furthermore, Zheng *et al.* have recently revealed that the metabolic reprograming during neuronal differentiation from aerobic glycolysis to oxidative phosphorylation was marked by the loss of two metabolic enzymes, namely HK2 and LDHA, and the alteration of pyruvate kinase.[27] Based on these previous studies, one may speculate that baicalein can direct neuronal differentiation of NSCs given its inhibitory effects on HK2 and LDHA. In central nervous system (CNS) diseases, baicalein has shown potent neuroprotective effects and promoted the recovery of traumatic CNS injury through various mechanisms, such as autophagy activation and inhibition of pyroptosis and endoplasmic reticulum-mediated apoptosis.[28–30] However, much less is known about the effects of baicalein on NSCs and on neurogenesis during the SCI repair.

Within this context, the present work aims to study the potential effects of baicalein on neuronal differentiation of NSCs and on nerve regeneration after SCI *in vivo*. Given that a small molecule is easily cleared by cerebrospinal fluid flow *in vivo*,[18] baicalein was loaded in fibrous collagen scaffolds in order to increase drug retention time and thus the baicalein-functionalized collagen scaffolds (BFCSs) were fabricated. Collagen, as the primary structural element of the extracellular matrix, was chosen due to its wide applications in the delivery of neurotropic factors and drug molecules in tissue engineering.[31,32] In addition, its biocompatibility and feasibility in SCI repair have been verified in our previous studies *in vivo* and in clinical trials.[18,33–35] Then, the physiochemical properties of the BFCSs with varied amounts of baicalein loaded were characterized, and their effects on neuronal differentiation were studied *in vitro* with isolated primary NSCs. Furthermore, the BFCSs with an optimized amount of baicalein loaded were transplanted in the lesion area of SCI rats. This allowed us to evaluate their roles in nerve regeneration in a complex inhibitory microenvironment, as well as the effects on functional recovery of injured animals.

Materials and methods

Materials and reagents

The chemicals used were all of analytical grade and purchased from Sigma Aldrich. The reagents used for cell experiments were purchased from Gibco Thermo Fisher Scientific. Antibodies were obtained from Abcam.

Preparation and characterization of the baicalein-functionalized collagen scaffolds (BFCSs)

Collagen derived from bovine corium (DB WUDEREGEN Biomedical Technologies (Jiangsu) Co., Ltd) was dissolved in 1% (v/v) acetic acid with a concentration of 30 mg mL^{-1}. To prepare the BFCSs, different amounts of baicalein were dissolved in 10 μL DMSO and mixed with 10 mL collagen solution. In order to ensure that a sufficient amount of baicalein is loaded and it has homogeneous distribution, DMSO was chosen as a solvent for baicalein because of its much lower solubility in aqueous solution than that in organic solvent. The mixed solutions were then pumped through a fine orifice of a spinneret into a coagulating bath containing 10 mM 1-ethyl-3-(3-dimethylaminopropyl)carbodiimide (EDC) and 10 mM *N*-hydroxysuccinimide (NHS) dissolved in PBS at room temperature, followed by incubation in the coagulating solution at 4 °C overnight. The continuous filaments were then collected using a take-up roller followed by freeze-drying for further use (see ESI Fig. S1A† for a schematic illustration of the BFCS preparation process). In order to determine the final amount of baicalein loaded in the BFCSs, the BFCSs were immersed in proteinase K solution at 56 °C for 10 min until the scaffold was completely dissolved. The solutions were then centrifuged at 14 000*g* for 15 min at room temperature and the supernatant was collected, followed by absorbance measurements at 277 nm. The BFCS without baicalein loaded was used as a control considering that proteinase K and the degraded collagen can cause a background during the measurement. The amount of baicalein was then calculated according to a standard curve of baicalein and the measurements were repeated 3 times with different batches of samples. The release kinetics of baicalein from the scaffolds was then measured according to a method reported in our previous study.[33] Briefly, in each group, the BFCS was immersed in PBS containing 0.2% Tween 80 (pH = 7.4) in an Eppendorf tube. The tube was placed in a shaker at 100 rpm and 37 °C. 50 μL solution was collected at different incubation times followed by the addition of 50 μL fresh PBS containing 0.2% Tween 80. The absorbance of the collected solution at 277 nm was then measured and the amount of baicalein released was calculated according to the standard curve. The experiment was repeated 3 times to confirm the reproducibility.

As a next step, the physical properties of the BFCSs were characterized. A scanning electron microscope (SEM) (Quanta

400 FEG, FEI) was used to characterize the morphology of the BFCSs, with the one loaded with 0.98 μg baicalein as a representative. Free-dried scaffolds were sputter-coated with gold at 35 mA for 3.5 min and observed under the thermal field emission SEM at 20 kV with images recorded. To evaluate the mechanical properties of the scaffolds, tensile tests were performed using an electronic universal testing machine (Instron 3365). Briefly, the baicalein collagen scaffolds of each group were fully wetted at room temperature, and the stress–strain value was detected. The sensor was set to 10 N, with a 20 mm min^{-1} lifting speed of the upper plate.

Isolation and culture of primary neural stem cells (NSCs)

In order to obtain primary neural stem cells (NSCs), the newborn rats purchased from Shanghai SLAC Experimental Animal Co., Ltd were rinsed with pre-cooled 75% ethanol and their telencephalons were dissected on ice. The collected tissues were washed once with pre-cooled PBS and cut into small pieces with a diameter around 5 mm, followed by digestion in 10 mL TrypLE Express at 37 °C with trituration every 5 min. After 20 min, the digestion reaction was stopped by the addition of 10 mL PBS and the dissociated cell suspension was filtered through a 40 μm mesh to remove undigested tissue blocks, followed by centrifugation at 350*g* for 5 min at room temperature. The obtained cells were then resuspended and cultured in DMEM/F12 medium supplemented with 20 ng mL^{-1} EGF, 20 ng mL^{-1} bFGF and 2% B27 (growth medium) under a humidified atmosphere containing 5% CO_2 at 37 °C. After 4 days in culture, NSCs were grown as free-floating neurospheres and were ready for the subsequent experiments.

NSC identification and differentiation

Neurospheres were collected by centrifugation at 150*g* for 5 min. The pellets were suspended in 5 mL TrypLE Express for 8 min at 37 °C followed by the addition of 5 mL PBS to stop the digestion reaction. NSCs were then dissociated by 20–30 rounds of pipetting. To validate the purity of the isolated NSCs, dissociated cells from neurospheres were resuspended in an attachment medium containing DMEM supplemented with 4.5 g L^{-1} glucose, 10% fetal bovine serum and 100 IU mL^{-1} penicillin, and seeded in a 35 mm dish precoated with 0.1 mg mL^{-1} poly-D-lysine. After 4 h, the attachment medium was replaced by the growth medium. At 24 h after cell seeding, immunostaining was applied to visualize the expression of nestin of the plated cells. Briefly, the cells were washed 3 times with PBS and fixed with 4% formaldehyde at room temperature. After 15 min, the cells were washed with PBS again, permeabilized with 0.5% Triton X-100 for 5 min and blocked in 5% bovine serum albumin for 1 h. The cells were then incubated with anti-nestin antibody (1 : 1000) overnight at 4 °C, followed by 3-times washing of PBS and incubation with Alexa Fluor 488-conjugated secondary antibody (1 : 5000) and 1 μg mL^{-1} DAPI in the dark for 30 min at 37 °C. The cells were then observed using a laser-scanning confocal fluorescence microscope (Olympus).

The differentiation of NCSs was studied in a 24-well plate and then on the BFCSs. To study the NSC differentiation in a 24-well plate, 7×10^4 cells dissociated from the neurosphere were dispersed in an attachment medium and seeded in each well precoated with 0.1 mg mL^{-1} poly-D-lysine in water. After 4 h, the attachment medium was replaced with a differentiation medium containing DMEM/F12 medium supplemented with 2% B27 and 100 IU mL^{-1} penicillin. The cells were then cultured under a humidified atmosphere containing 5% CO_2 at 37 °C and half of the differentiation medium was refreshed every 2 days. To study the effects of baicalein on NSC differentiation, the differentiation medium containing different concentrations of baicalein (0–500 nM) was added after cell attachment. Similarly, to study the differentiation of the NSCs on the BFCSs, 4 mg of the scaffold in each group was sterilized under UV for 12 h and incubated in 1 mg mL^{-1} laminin solution at 4 °C overnight followed by 3 washes with PBS. The pretreated scaffolds were placed in a 24-well plate and 7×10^4 NSCs per well dispersed in an attachment medium were added. After a 7-day culture, the differentiation of the NSCs seeded in a pretreated 24-well plate or on the BFCSs was studied by immunostaining of beta III Tubulin (Tuj-1) (1 : 1000) and glial fibrillary acidic protein (GFAP) (1 : 1000). For the latter one, the filaments containing stained cells from each group were placed on a glass slide. The cells were observed using a laser-scanning confocal fluorescence microscope. Experiments on each group were repeated 3 times to confirm the representability, and the number of DAPI-positive cells, Tuj-1 positive cells, and GFAP positive cells and axonal length were analysed respectively.

Ethical statement

All animal procedures were performed in accordance with the Guidelines for the Care and Use of Laboratory Animals from the National Institutes of Health and approved by the Ethics Committee of Suzhou Institute of Nano-Tech and Nano-Bionics, Chinese Academy of Sciences, Suzhou, China.

Animal care and surgery

Female Sprague Dawley rats (180–200 g) were purchased from Shanghai SLAC Experimental Animal Co., Ltd. A rat model of completely transected spinal cord injury (SCI) was established according to our previous studies.[18,33] Briefly, rats were anesthetized by an intraperitoneal injection of 2% pentobarbital sodium in normal saline (0.15 mL per 100 g). The vertebrae at the T7–T9 level were then exposed by making a 4 cm midline incision. Dorsal laminectomy was then conducted and the spinal cord tissue with a length of 4 mm at the T8 segment was completely removed. Gelfoam was immediately placed in the lesion area for hemostasis. Each group of the fibrous BFCSs containing varied amounts of baicalein with a weight of 4 mg and a length of 4 mm were implanted in the lesion gap bridging the transected sites. Musculature and skin were sutured successively, and wounds were disinfected with iodine tincture. The rats after surgery were administered antibiotics intraperitoneally once per day for one week. Manual bladder

expression was performed for the SCI rats twice per day until their bladder reflexive function was observed.

Immunohistochemical and histological analyses

After 1 week or 8 weeks post-surgery, rats were anesthetized and transcardially perfused with PBS for 5 min and 4% paraformaldehyde for another 5 min. Fixed spinal cord tissues were then incubated in 4% paraformaldehyde at 4 °C overnight, followed by dehydration with 20% sucrose at 4 °C for 24 h and 30% sucrose at 4 °C overnight in turn. Dehydrated tissues were then frozen in a Tissue Tek O.C.T. compound (Sakura Finetek) and cryo-sectioned longitudinally with a thickness of 12 μm. Tissue sections were stored at −20 °C for further use.

For immunohistochemical analysis, tissue sections were rinsed once with PBS, followed by permeabilization with 0.5% Triton X-100 for 5 min and 1 h incubation in goat serum at room temperature. Primary antibodies diluted in PBS were then incubated with sections at 4 °C overnight, which included anti-GFAP (1 : 200), anti-Tuj-1 (1 : 1000), anti-NeuN (1 : 1000), anti-ChAT (1 : 1000) and anti-NF (1 : 1000). Tissue sections were then washed 3 times with PBS and incubated with Alexa Fluor conjugated secondary antibodies in the dark at room temperature. After 2 h incubation and 3 times of PBS wash, a mounting medium containing 4,6-diamidino-2-phenyl indole (DAPI) was used to mount the stained sections. Images were captured using a confocal microscope. To quantify the proportion of positively immunostained cells, the total cell number in the lesion area was first calculated based on the DAPI positive cells by using ImageJ software (https://www.fiji.sc). Then, the number of cells positively stained by different antibodies in the injury site were manually counted and their percentage to total cells was calculated. To quantify the signal of GFAP positive cells at the lesion border, because of a dense distribution of astrocytes, the average fluorescence intensity of the GFAP signal was measured with that of the DAPI signal as a control. In addition, for histological studies, tissue sections from each group were stained with a hematoxylin and eosin (H&E) kit and observed using a Leica SCN400 slide scanner.

Evaluation of motor functional recovery

After surgery, the hindlimb's functional recovery in SCI rats was assessed every 7 days for 8 weeks, according to the Basso–Beattie–Bresnahan (BBB) locomotor rating scale with a score from 0 (no movement) to 21 (normal gait). Briefly, the rats were placed in an open field (120 × 200 cm) and the movement of their hindlimbs was observed. The assessment was performed by 3 researchers blinded to the group and the score for every rat at each time point was the average from all observers.

Data analysis

All data were presented as the average and standard deviation over at least 3 replicates. Statistical analysis was performed using GraphPad Prism 9. The statistical difference between two groups was assessed using Student's *t*-test. For the comparison of multiple groups, one-way ANOVA was used. A significance level of 5% was used. $p < 0.05$, $p < 0.01$ and $p < 0.001$ were considered significant, highly significant and extremely significant, respectively, and indicated separately with *, ** and ***.

Results and discussion

Effects of baicalein on neuronal differentiation of neural stem cells (NSCs)

Primary NSCs were isolated from the hippocampus of newborn rats, and their purity and differentiation capacity were identified (ESI Fig. S2†). To evaluate the effects of baicalein on neuronal differentiation of NSCs, dissociated NSCs were cultured in a differentiation medium and incubated with a series of concentrations of baicalein for 7 days, followed by immunostaining of beta III Tubulin (Tuj-1), a marker of newborn immature neurons, and glial fibrillary acidic protein (GFAP), a marker of astrocytes. As shown in Fig. 1, with increased concentration of baicalein from 0 nM to 100 nM, more Tuj-1 positive cells were observed and their percentages were significantly raised from 31.16 ± 6.94% in the control group to 48.23 ± 3.96% in the group with 100 nM baicalein treatment. In contrast, the number of GFAP positively stained cells were gradually decreased, with 6.49 ± 1.69% GFPA + cells

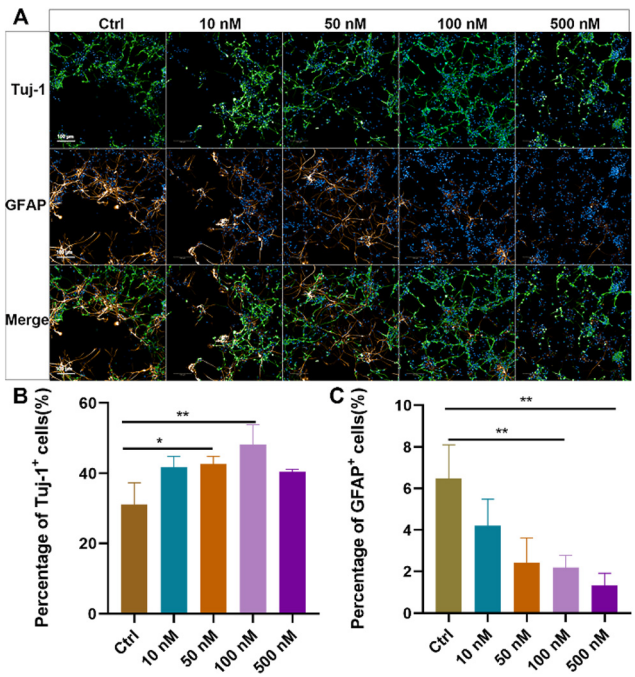

Fig. 1 Effects of baicalein on NSC differentiation. (A) Representative microscopy images of Tuj-1 positive cells (in green) and GFAP positive cells (in yellow) differentiated from NSCs after 7-day culture with different concentrations of baicalein. Nuclei were visualized by DAPI staining (in blue). Scale bar: 100 μm. (B and C) Quantification of the percentage of Tuj-1 positive cells (B) and GFAP positive cells (C) in DAPI positively stained cells per visual field. Data are the mean and standard deviation over 3 replicated experiments. Statistical difference between the control and each baicalein treated group was analysed by Student's *t*-test.

in the control and only 2.19 ± 0.67% in the 100 nM baicalein treated group. However, when the baicalein concentration was further increased to 500 nM, both Tuj-1 positive and GFAP positive cell numbers were decreased, which might be due to the cellular toxicity induced by a high drug dose. Altogether, the *in vitro* study suggested that baicalein at a low concentration range can facilitate neuronal differentiation of NSCs and reduce their differentiation into astrocytes, indicating its potential therapeutic effects in spinal cord injury (SCI) repair.

Construction and characterization of the baicalein-functionalized collagen scaffolds (BFCSs)

After verifying the promotion effects of baicalein on neuronal differentiation, we further applied it to SCI treatment. However, baicalein as a small molecule (see its chemical structure in Fig. 2A) is easily cleared by the cerebrospinal fluid flow once injected in the lesion area of spinal cords. Thus, in order to avoid rapid clearance and achieve a local and sustained release of baicalein during SCI repair, baicalein-functionalized collagen scaffolds (BFCSs) were developed through mixing baicalein in collagen solution followed by wet-spinning and freeze-drying (Fig. 2B; see the Materials and methods for details of BFCS preparation and ESI Fig. S1B† for an optical image of the prepared scaffolds). The loading amount of baicalein in the BFCSs was then determined. As listed in Fig. 2C, a series of BFCSs with different drug contents were obtained, including 0.00 μg, 0.98 μg, 1.10 μg, 1.40 μg and 5.00 μg baicalein loaded BFCSs (4 mg scaffold of each group), which were used for the following *in vitro* and animal studies. Among different BFSCs, the collagen scaffold without baicalein loaded (0.00 μg) was used as the control group for their physicochemical characterization, as well as for the following *in vitro* and *in vivo* experiments. It has been reported that 10 μg baicalein administered intrathecally can attenuate inflammatory hyperalgesia without causing overt toxicity in rats,[36] suggesting the safety of the obtained BFCSs with maximum 5.00 μg baicalein loaded for the following animal studies. The release rate of baicalein from the BFCSs was measured by exposure in PBS containing 0.2% tween-80 (Fig. 2D).[33] For different BFCSs, around 30% of baicalein were released in the first hours followed by a gradual drug release over time. After 120 h (5 days), 0.98–1.40 μg baicalein loaded in the BFCSs was completely released, while the 5.00 μg baicalein loaded BFCS showed a slower cargo release rate with 30% of the cargo retained even after 168 h (7 days) exposure. Our previous studies have discovered that in SCI animals endogenous NSCs start to migrate to the lesion sites once injury occurs, and massively proliferate since day-3 post-injury reaching a peak amount at day-5 after SCI.[10,11] Thus, baicalein sustainably released from the BFCSs for at least 5 days can benefit the NSCs arriving at the injured area, which indicates a match of the drug release profile of the BFCSs to the time frame of neurogenesis in SCI animals.

Next, the morphology and mechanical properties of the BFCSs were characterized. For morphology measurements by scanning electron microscopy (SEM), the control and BFCS with 0.98 μg baicalein loaded as a representative showed a similar microstructure with arrayed channels (Fig. 1E), consistent with the morphology of the fibrous collagen used in our previous studies.[18,33] To characterize the mechanical properties of the BFCSs, tensile tests were performed. As shown in Fig. 1F and G, the obtained BFCSs with different amounts of baicalein loaded displayed typical stress–strain curves of viscoelastic materials with similar Young's modulus, indicating that the mechanical properties of collagen scaffolds were not

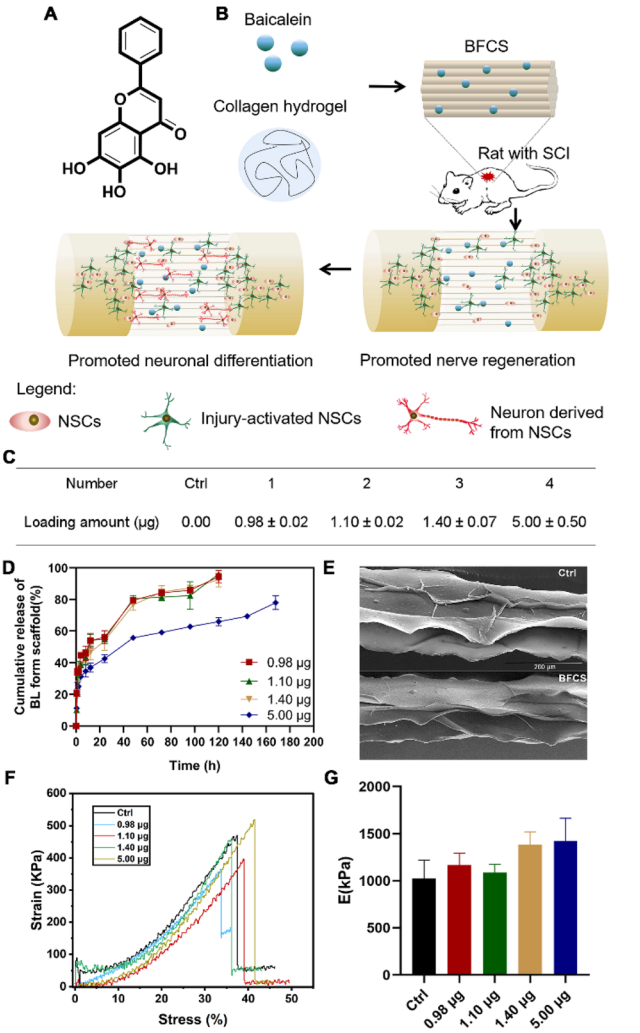

Fig. 2 Construction and characterization of the BFCSs. (A) Chemical structure of baicalein. (B) Schematic illustration of the BFCS preparation and their effects to promote neuronal differentiation in SCI rats. (C) The amount of baicalein loaded in the BFCSs with a mass of 4 mg and a length of 4 mm in each group. The data are presented as the mean and standard deviation over 3 measurements of each group. (D) Drug release kinetics of the BFCSs loaded with different amounts of baicalein in PBS containing 0.2% tween-80 over 7 days. Data are the mean and standard deviation over 3 replicates. (E) Representative SEM images of the control and BFCS containing 0.98 μg baicalein. (F) Stress–strain curves of the BFCSs loaded with different amounts of baicalein in a representative measurement. (G) Young's modulus of the BFCSs. Data are the mean and standard deviation over 3 measurements. One-way ANOVA was performed and the results indicated that the difference across groups was not statistically significant ($p < 0.05$ was considered significant).

affected by a payload of baicalein. Thus, the obtained BFCS can release baicalein in a sustained manner and, at the same time, possessed similar mechanical properties and morphology to collagen, which can provide sufficient physical supports for cellular activity in the subsequent *in vitro* and *in vivo* studies.

Effects of the BFCSs on NSC differentiation

The obtained BFCSs were then assessed for their biocompatibility and roles in neuronal differentiation. Dissociated NSCs were seeded on the BFCSs in a differentiation medium and identified after 7-day culture by immunostaining of Tuj-1 and GFAP. As shown in Fig. 3A, the cells were distributed along fibrous scaffolds with Tuj-1 or GFAP positively stained in different groups. The percentage of Tuj-1 and GFAP positive cells on the filaments in each group was then calculated (Fig. 3B and C). Compared to the control group which contained only 30.81 ± 1.46% Tuj-1 positive cells, a significantly higher percentage of Tuj-1 positive cells was observed in the BFCSs loaded with 0.98 μg, 1.10 μg and 1.40 μg baicalein (with 43.20 ± 2.78%, 45.59 ± 2.99% and 45.46 ± 4.17% of Tuj-1 positive cells in the respective group). However, when the amount of baicalein in the BFCSs increased to 5.00 μg, the proportion of the Tuj-1$^+$ cells decreased to 26.98 ± 1.10%. Meanwhile, significantly lower percentages of GFAP positive cells were observed in the BFCSs containing 0.98 μg and 1.10 μg baicalein (with 24.85 ± 5.14% and 28.67 ± 4.92% of GFAP positive cells, respectively) in comparison with the control (with 38.31 ± 1.20% of GFAP positive cells), but no obvious difference was observed in the groups with 1.40 μg and 5.00 μg baicalein loaded. These results indicated that, consistent with the effects of baicalein on NSC differentiation (Fig. 1), the obtained BFCSs, especially with a low amount of baicalein loaded (0.98–1.10 μg), can regulate and promote the differentiation of NSCs into neurons and reduce the production of astrocytes.

Moreover, the axon length of the Tuj-1 positively stained cells was measured in each group. Surprisingly, we discovered that the BFCSs with 0.98–1.40 μg baicalein loaded can not only promote neuronal differentiation (Fig. 3B), but also have a positive effect on axon elongation (Fig. 3D). In the control group the length of the axon was 41.38 ± 8.66 μm, while in the group of the BFCSs containing 0.98 μg, 1.10 μg and 1.40 μg baicalein, the axons significantly grew to 76.18 ± 8.36 μm, 85.85 ± 7.38 μm and 73.98 ± 11.02 μm, respectively. It has been reported that the oriented microstructure of a scaffold mimicking the biological architecture of spinal cord tissues can guide axon growth and is advantageous in nerve fiber extension.[37,38]

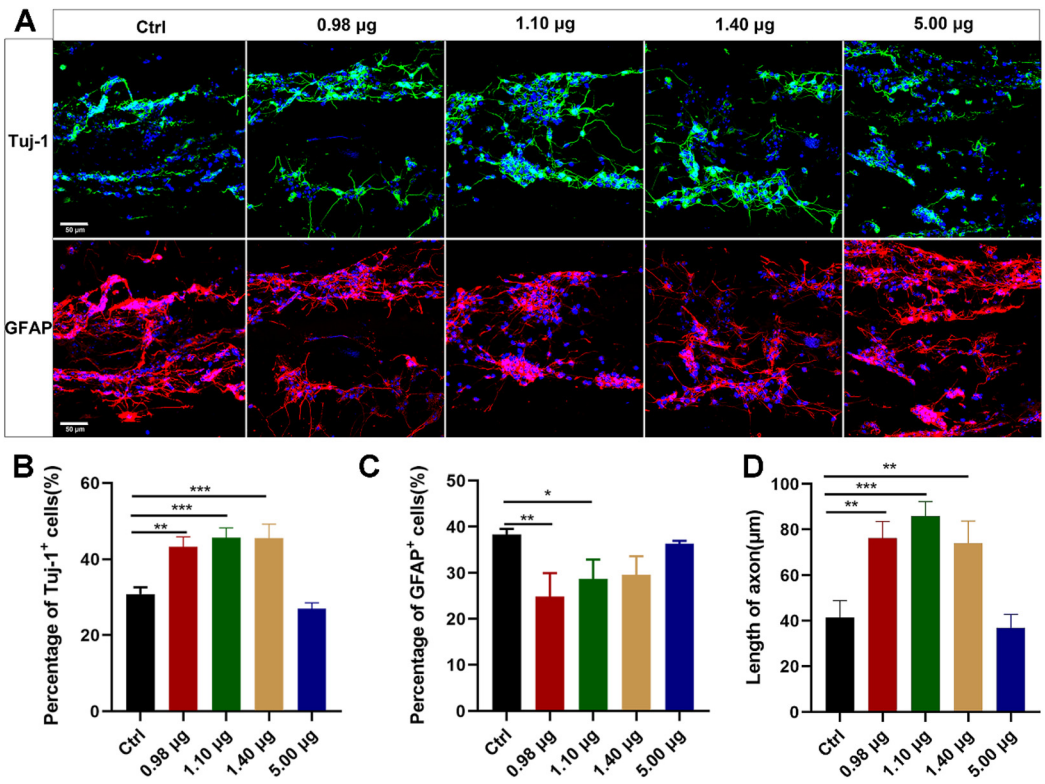

Fig. 3 *In vitro* studies of neuronal differentiation of the NSCs on the BFCSs. (A) Representative microscopy images of NSCs seeded on the BFCSs with varied amounts of baicalein for 7 days in a differentiation medium. Cells were stained with Tuj-1 (green), GFAP (red) and DAPI (blue) to visualize the differentiated neurons, astrocytes and their nuclei, respectively. Scale bar: 50 μm. (B–D) Quantification of the percentage of Tuj-1 positive cells (B), GFAP positive cells (C) and axon length (D) in DAPI positively stained cells seeded on BFCSs per filament after a 7-day culture in a differentiation medium. The data are the mean and standard deviation over 3 replicated experiments. Student's *t*-test was used in panels (B–D) separately to analyse the statistical difference between the control and other treatment groups.

Thus, we speculated that the baicalein loaded and the fibrous collagen matrix of the BFCSs had a synergistic effect on nerve regeneration. The former component promoted NCS differentiation into neurons and the latter one subsequently guided the axon extension.

Effects of the BFCSs on neuronal differentiation and functional neuronal regeneration in SCI rats

As a next step, the effects of the BFCSs on neuronal differentiation *in vivo* were evaluated. A rat model of completely transected SCI was established, and the fibrous BFCSs with a length of 4 mm and a weight of 4 mg were transplanted immediately in the lesion site (ESI Fig. S3†). Our previous studies have reported the activation of endogenous NSCs after SCI and their gradual migration to the injured centre with a peaking amount at 5 days post-injury.[39,40] Thus, we first analysed if the treatment of the BFCSs can induce neuronal differentiation of NSCs around the lesion site by Tuj-1 staining in a short term at 1-week post-surgery. As shown in Fig. 4, compared to the control group with 0.80 ± 0.07% Tuj-1 positive cells, a significantly higher percentage of Tuj-1 was observed in the SCI rats transplanted with the BFCSs containing 0.98 μg and 1.10 μg baicalein, which included 1.67 ± 0.18% and 1.75 ± 0.72% Tuj-1 positive cells, respectively. However, there was no obvious difference in the ratio of Tuj-1 positive cells between the treatment groups with a higher amount of baicalein (1.40 μg and 5.00 μg) and the control. In line with the *in vitro* study of the BFCSs (Fig. 3), the animal study at 1-week post-surgery suggested that a low dose of baicalein (0.98–1.10 μg) loaded in the BFCSs promoted neural differentiation, while no obvious effects were observed in the groups containing higher amounts of baicalein (1.40 μg and 5.00 μg). We noticed that the percentage of the Tuj-1 positive cells in all the treatment groups remained low (less than 3%), which was probably because the neurogenesis process in SCI animals typically proceeds for months, indicating the necessity of a long-term *in vivo* study.[41,42]

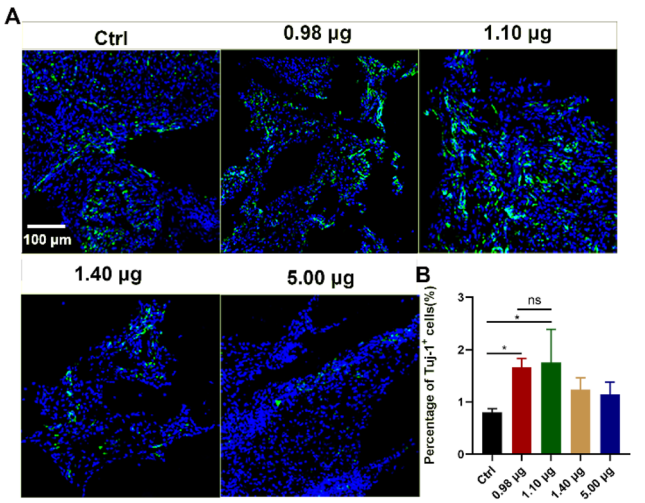

Fig. 4 Evaluation of the newborn immature neurons in the injured centre of spinal cords at 7 days post-surgery. (A) Representative microscopy images of the injured area of the spinal cords transplanted with the BFCSs. Spinal cord tissues were stained with DAPI (blue) and Tuj-1 (green) to visualize the cell nuclei and immature neurons, respectively. Scale bar: 100 μm. (B) Quantification of the percentages of Tuj-1 positive cells in the lesion center of the spinal cords. Experiment of each group was performed with at least 3 rats to confirm the reproducibility and the Tuj-1 positive cells in the whole lesion area per rat were counted. Data are the mean and standard deviation over replicates. The statistical difference between the control and other treatment groups was analysed by Student's *t*-test.

Therefore, the effects of the BFCSs on neurogenesis in SCI rats were further evaluated at 8 weeks post-surgery, when the SCI recovery process was relatively more completed. Both the *in vitro* and short-term *in vivo* studies have shown that low doses of baicalein (0.98–1.10 μg) loaded in the BFCSs can efficiently induce neuronal differentiation (Fig. 3 and 4). Though a slightly higher proportion of Tuj-1 positive cells was observed in the group of the BFCSs containing 1.10 μg baicalein than the one with 0.98 μg baicalein *in vitro* and *in vivo*, there was no significant difference in the differentiation-promoting effects between the two groups (ESI Fig. S4†). Thus, in order to avoid potential side effects during administration, we took the BFCS containing a lower dosage (0.98 μg instead of 1.10 μg baicalein) as an optimum condition for the long-term *in vivo* study. Meanwhile, we asked if a lower amount of drug than 0.98 μg baicalein loaded in the BFCS (used as the optimum condition) can even further promote neurogenesis. To gain more information on the dose–response effects of baicalein on NSCs with a wider dosage range and to understand the optimum dosage for the SCI treatment, in the long-term animal experiment, the BFCS loaded with a lower dose of baicalein (0.40 μg) was introduced as an additional experimental group, together with the one containing a higher amount of baicalein (1.40 μg) for comparisons. Their drug release kinetics and mechanical properties were compared and are shown in ESI Fig. S5.† As shown in Fig. 5A, as expected, the number of Tuj-1 positive cells in the lesion site at 8 weeks post-injury increased. Among different treatment groups, the injured tissue transplanted with the BFCSs containing 0.40 μg and 0.98 μg baicalein showed a significantly higher percentage of Tuj-1 positive cells (30.64 ± 5.37% and 24.04 ± 1.25%, respectively) than the control group (13.00 ± 1.36%) (Fig. 5A and E). Meanwhile, the presence of mature neurons and axonal regeneration were studied by immunostaining of NeuN and neurofilament (NF) separately (Fig. 5B–C and F–G). A larger number of NeuN positive cells was observed in the lesion area of the spinal cords treated with BFCSs containing 0.98 μg baicalein, which accounted for 1.44 ± 0.15% of DAPI stained cells and showed a significant difference from other treatment groups (Fig. 5B and F). For the NF staining, the percentage of positive cells in the groups of the BFCSs containing 0.40 μg and 0.98 μg baicalein was more than 4 times higher than that of the control (Fig. 5C and G). In addition, we further studied whether the differentiated neurons in the lesion area can mature into functional neurons, such as sensory neurons. By immunostaining of the spinal cord tissue with ChAT, a cholin-

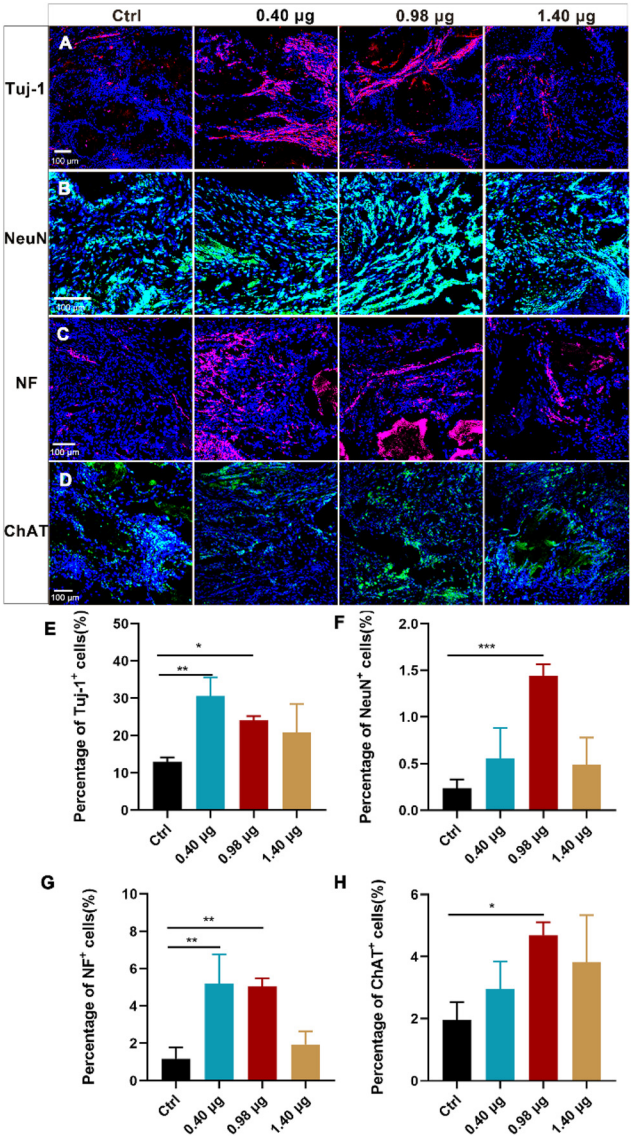

Fig. 5 Evaluation of neuron regeneration in the injured centre of spinal cords treated with different BFCSs at 8 weeks post-SCI. (A–D) Representative immunofluorescence images of the spinal cord tissues stained with Tuj-1 (A), NeuN (B), NF (C) and ChAT (D). Cells were stained with DAPI (in blue) to visualize the nuclei. Scale bar: 100 μm. (E–H) Quantitative analysis of the percentages of Tuj-1 (E), NeuN (F), NF (G), and ChAT (H) positive cells in DAPI positively stained cells in the injured area according to the corresponding immunostaining images. Experiments of each group of the BFCSs were performed with minimum 3 SCI rats to confirm the reproducibility. Data are presented as mean and standard deviation over replicated experiments. The statistical difference between the control and other treatment groups was analysed by Student's *t*-test.

ergic neuron marker, we discovered a significantly larger portion of positive cells in the group treated with BFCSs containing 0.98 μg baicalein (4.69 ± 0.48%) compared to other treatment groups (Fig. 5D and H).

Altogether, the immunofluorescence imaging (Fig. 5A–D) and the corresponding quantitative analysis (Fig. 5E–H) showed that the transplantation of the BFCSs loaded with 0.98 μg baicalein can efficiently enhance neuron generation including newborn, mature and functional ones in the lesion sites after 8 weeks post-injury, which was consistent with the results obtained from the *in vitro* and short-term *in vivo* studies (Fig. 3 and 4). Moreover, in the *in vitro* study we discovered that the BFCSs with a small amount of baicalein loaded can facilitate not only neuronal differentiation but also axon elongation (Fig. 3). This effect was further confirmed by immunostaining of NF in the long-term *in vivo* study, which showed a significantly higher portion of NF positively stained cells in the group treated with 0.40 μg and 0.98 μg baicalein loaded BFCSs (Fig. 5C and G). Meanwhile, these results also

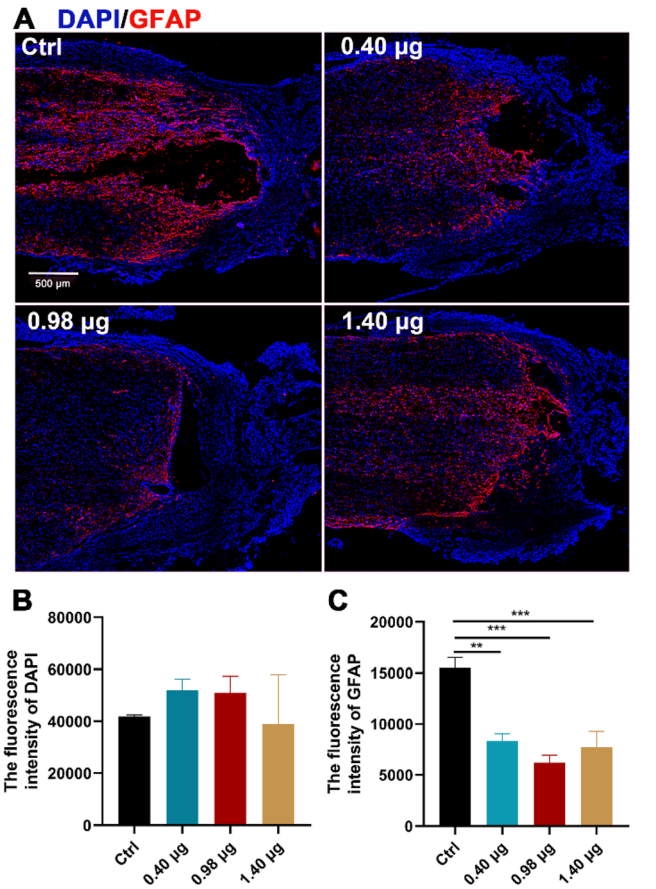

Fig. 6 Astrocyte identification at the lesion edge of the spinal cords treated with the BFCSs at 8 weeks post-surgery. (A) Representative immunofluorescence images of spinal cords treated with the BFSCs containing different amounts of baicalein in the injured edge. Cells were stained with GFAP (in red) and DAPI (in blue) to visualize reactive astrocyte distribution and nuclei, respectively. Scale bar: 500 μm. (B and C) Quantification of the average fluorescence intensity of DAPI (B) and GFAP (C) in each treatment group. We noticed that astrocytes distributed densely at the lesion border, which was difficult for quantifying positively staining cells. Thus, instead, the average fluorescence intensity was measured. Experiments of each group were performed using at least 3 SCI rats and data are presented as mean and standard deviation over replicates. The statistical difference between the control and other treatment groups was analysed by Student's *t*-test.

indicated that a low dose of baicalein, instead of a higher one (1.40 μg in the BFCS), had a positive role in nerve regeneration *in vivo*.

It has been reported by several studies that baicalein has potent neuroprotective effects in central neural system (CNS) injury by multiple pharmacological activities, such as anti-apoptotic, antioxidant, anti-inflammatory and anti-excitotoxicity activities.[20–22] In order to disentangle increased neurogenesis after the BFCS implantation due to the neuroprotective effects of baicalein or those from promoted differentiation of NSCs, the population of the astrocytes at the lesion border in each treatment group was examined by immunostaining of GFAP. As shown in Fig. 6A and B, the mean fluorescence intensity of DAPI in the measured area was comparable in different treatment groups. However, when assessing the expression of GFAP, a strong GFAP signal was observed at the lesion edge of spinal cords in the control (15504 ± 726), while the fluorescence intensity was significantly reduced in the groups treated with the BFCSs containing 0.40 μg, 0.98 μg, and 1.40 μg baicalein, among which the group with 0.98 μg baicalein as an optimum condition showed the lowest value (6191 ± 870) (Fig. 6A and C). It is well known that NSCs tend to differentiate into astrocytes because of the presence of an inhibitory microenvironment after SCI.[15–17] The reduced GFAP expression in the SCI rats was in line with the observations *in vitro* (Fig. 3) that a low dose of baicalein (0.98 μg) loaded in the BFCSs can direct NSC differentiation and inhibit astrocyte production. This explained the neurogenesis effects of the BFCSs *in vivo* – at least partially – resulting from neuronal differentiation of NSCs.

Tissue regeneration and motor functional recovery evaluation

In order to evaluate the tissue regenerative effects, injured spinal cords with different treatments were dissected at 8-week post-surgery, and tissue cables connecting the entire 4 mm long transection gap of the spinal cords were observed in all groups (Fig. 7A). The histological changes of the injured tissue in different treatment groups were then further studied by hematoxylin and eosin (H&E) staining. As shown in Fig. 7B, in the control group, the injured tissue remained disconnected with a few cells distributing in the lesion area. In contrast, in the treatment group of the BFCS containing 0.98 μg baicalein, a larger number of cells across the transection gap bridging the rostral and caudal spinal cords was observed with an obviously reduced area of the lesion cavity. The results indicated that the BFCSs with 0.98 μg baicalein loaded not only accelerated neurogenesis but also promote the tissue regeneration with transected spinal cord re-bridged and tissue integrating.

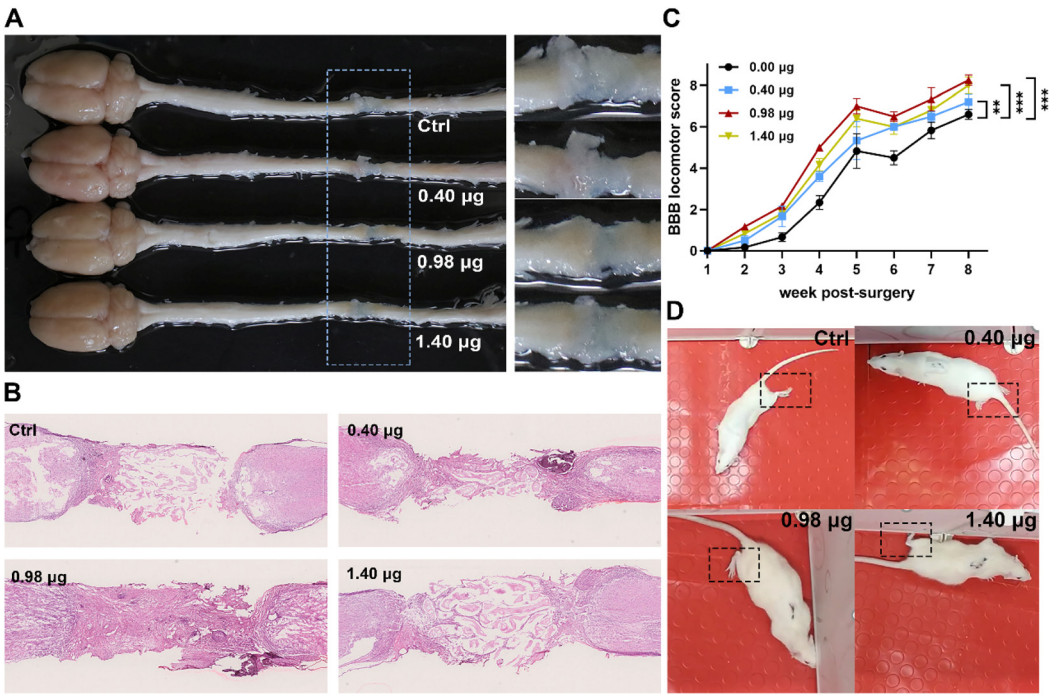

Fig. 7 Evaluation of tissue regeneration and motor functional recovery of the SCI rats treated with the BFCSs. (A) Representative image of the gross morphology of spinal cords dissected from SCI rats in different treatment groups. To clearly show the regenerative tissue cables, parts of the picture containing lesion sites were zoomed in and displayed in the right panel. (B) Representative images of longitudinal H&E staining of spinal cords of SCI rats in each group after 8-week post-injury. (C) BBB scores of hindlimb locomotion of SCI rats in each group during 8 weeks after SCI. For assessing the functional recovery of SCI rats, 4–6 rats per treatment group at each time point were examined. The data are mean and standard deviation over replicates. The statistical difference of the BBB scores between the control and other treatment groups was analysed by paired *t* test. (D) Representative images of the SCI rats in each treatment group during their movement in an open field at 8-weeks post-surgery. Corresponding videos are provided in ESI Videos S1–S4.†

Meanwhile, the motor function of the SCI rats treated in different treatment groups was assessed weekly from the first to the eighth week post-injury using the Basso–Beattie–Bresnahan (BBB) locomotor scale. A complete hindlimb paralysis of the rats (BBB score = 0) was observed in all groups in the first week, and their motor function of the lower limbs gradually recovered with BBB scores slowly increasing over time (Fig. 7C). Among the different treatment groups, the rats transplanted with the BFCS containing 0.98 μg baicalein achieved the highest BBB scores at each measurement time point, showing a significant difference when compared to the control group during 8 weeks observation (Fig. 7C). At the last measurement time point (week-8 post-injury), the movement of the SCI rats in each group was recorded (Fig. 7D and the corresponding videos in ESI Video S1–S4†). We observed that the rats in the control group dragged hind legs during their movement, while the hindlimbs of the rats treated with the BFCSs containing 0.40–1.40 μg baicalein could automatically move and showed knee joint and ankle joint bending. Furthermore, the rats treated with 0.98 μg baicalein loaded BFCS displayed toe joint bending in the hindlimbs, which even can support the body. Overall, these results suggested that the BFCS transplantation facilitated motor functional recovery of the SCI rats, especially the group containing 0.98 μg baicalein in which the rats showed the most flexible movement.

Conclusions

Growing evidence has shown the great potential of NSCs in SCI repair due to their capacity to differentiate into neurons followed by circuit reconstruction.[6,7] However, because of the existence of an inhibitory microenvironment, NSCs around the lesion area tend to differentiate into astrocytes, which are subsequently involved in the glial formation and further hamper tissue regeneration,[13,15–17] suggesting high demands for strategies to direct neuronal differentiation. In the current work, inspired by the similarity of the metabolic pathway in the process of neuronal differentiation from NSCs and that involved in the cancer treatment induced by baicalein, a clinical drug, we studied the effects of baicalein on NSC differentiation and discovered that a low concentration of baicalein (50–100 nM) can enhance the neuronal differentiation of NSCs and inhibit their differentiation into astrocytes (Fig. 1). Based on this observation, a series of BFCSs containing different amounts of baicalein were prepared and applied to neurogenesis studies *in vitro* and in SCI rats. The BFCSs released the drug in a sustained way, thus avoiding a rapid clearance of baicalein by the cerebrospinal fluid flow during SCI treatment, and possessed a similar morphology and mechanical properties to the fibrous collagen reported in our previous studies (Fig. 2). In the *in vitro* study, the BFCSs contained a small amount of baicalein (0.98 μg–1.10 μg in 4 mg scaffolds) not only - in line with the previous observation – facilitated neuronal differentiation but also promoted axonal elongation probably due to a guidance effect of the fibrous scaffolds (Fig. 3). When implanted into the SCI rats, neurogenesis was clearly observed in the group treated with BFCSs containing 0.98 μg baicalein, with a larger portion of newborn, mature and functional neurons distributed in the lesion site (Fig. 4 and 5). More importantly, the BFCSs, especially the one with 0.98 μg baicalein loaded, improved tissue regeneration and integrity and motor functional recovery of the SCI rats (Fig. 7).

Strategies to induce neuronal differentiation have been widely explored in the past decades and several of them have been reported and used for the SCI treatment.[19] For example, our previous study has discovered that the microtubule-stabilizing agent paclitaxel can rescue myelin-inhibited neuronal differentiation, and thus a functional collagen scaffold with paclitaxel-encapsulated liposomes loaded was developed, showing beneficial effects in SCI repair.[18] Also, in order to block the epidermal growth factor receptor (EGFR)-mediated signalling activation that induces NSC differentiation into glial lineage, cetuximab, as an EGFR neutralizing antibody, was modified on the collagen matrix and this functionalized scaffold enhanced neuronal differentiation of NSCs at the lesion site and promoted functional recovery of SCI rats.[43,44] In the present study, for the first time, we proposed a potential strategy of metabolic modulation in directing neuronal differentiation for SCI repair, on the ground of a similarity of metabolic reprograming required for neuronal differentiation in NSCs and that induced by baicalein in cancer cells in order to reverse their chemoresistance.[23–26] Though the promotion effects of baicalein on neurogenesis were clearly observed *in vitro* and in SCI rats, further studies are needed to disclose the concrete mechanism and key biomolecules involved in NSC differentiation. Meanwhile, it will be interesting to compare the promotion efficiency of NSC differentiation induced by baicalein and other widely used reagents, such as small molecules and neurotropic factors, and different molecules redirecting neuronal differentiation based on varied mechanisms could be combined together for more efficient SCI treatments. In addition, we discovered that a high dose of baicalein did not contribute to neuronal differentiation. Thus, more work is required to understand these dose–response effects of baicalein on NSCs and to determine an optimum dosage for the SCI treatment. Moreover, it is known that baicalein possesses a neuroprotective property with – for instance – anti-apoptotic and anti-inflammatory effects among others.[20–22] Although the reduction of glial scar formation provided evidence that neurogenesis is specifically promoted (Fig. 6), it would be interesting in future studies to disentangle the contributions of baicalein in SCI repair of injured animals with their different pharmacological activities.

In conclusion, in this study, we discovered a promotion effect of baicalein on neuronal differentiation and thus baicalein-functionalized collagen scaffolds were developed for the SCI treatment. The application of the BFCSs provided an additional strategy for neurogenesis in the SCI repair, which might open up interesting possibilities in tuning the metabolic pathway of NSCs for CNS injury treatment.

Author contributions

Conceptualization, L. Q.; data curation, L. Q. and K. Y.; formal analysis, L. Q. and K. Y.; methodology, L. Q., L. Z., H. Z., L. Z. Q. and Y. Z.; investigation, L. Q., X. L., Y. C. and W. H.; writing – original draft, L. Q. and K. Y.; visualization, L. Q. and K. Y., writing – review & editing, K. Y., Y. C. and J. D.; validation, K. Y. and Y. C.; supervision, Y. C. and J. D.; resources, Y. C. and J. D.; funding acquisition, K. Y., Y. C. and J. D.; all authors have read and agreed to the published version of the manuscript.

Conflicts of interest

There are no conflicts to declare.

Acknowledgements

This work was supported by grants from the Major Program of National Natural Science Foundation of China (No. 81891002), the National Key Research and Development Program of China (No. 2021YFC2701403), and the Strategic Priority Research Program of the Chinese Academy of Sciences (No. XDA16040700). K. Y. kindly acknowledges the Chinese Academy of Sciences for additional funding (CAS Special Research Assistant Funding Program).

References

1 C. Darian-Smith, *Neuroscientist*, 2009, **15**, 149–165.
2 N. A. Silva, N. Sousa, R. L. Reis and A. J. Salgado, *Prog. Neurobiol.*, 2014, **114**, 25–57.
3 T. R. Ham and N. D. Leipzig, *Biomed. Mater.*, 2018, **13**, 024105.
4 F. M. Bareyre and M. E. Schwab, *Trends Neurosci.*, 2003, **26**, 555–563.
5 C. H. Tator, *Neurochirurgie*, 1991, **37**, 291–302.
6 H. Kumamaru, K. Kadoya, A. F. Adler, Y. Takashima, L. Graham, G. Coppola and M. H. Tuszynski, *Nat. Methods*, 2018, **15**, 723–731.
7 S. A. Goldman, *Cell Stem Cell*, 2016, **18**, 174–188.
8 Y. Rong, W. Liu, J. Wang, J. Fan, Y. Luo, L. Li, F. Kong, J. Chen, P. Tang and W. Cai, *Cell Death Dis.*, 2019, **10**, 340.
9 E. J. Lee, Y. Choi, H. J. Lee, D. W. Hwang and D. S. Lee, *J. Nanobiotechnol.*, 2022, **20**, 198.
10 X. Li, Y. Zhao, S. Cheng, S. Han, M. Shu, B. Chen, X. Chen, F. Tang, N. Wang, Y. Tu, B. Wang, Z. Xiao, S. Zhang and J. Dai, *Biomaterials*, 2017, **137**, 73–86.
11 C. Fan, X. Li, Z. Xiao, Y. Zhao, H. Liang, B. Wang, S. Han, X. Li, B. Xu, N. Wang, S. Liu, W. Xue and J. Dai, *Acta Biomater.*, 2017, **51**, 304–316.
12 Y.-T. Wang and H. Yuan, *Ibrain*, 2022, **8**, 199–209, DOI: **https://doi.org/10.1002/ibra.12048**.
13 C. Liu, L. Fan, J. Xing, Q. Wang, C. Lin, C. Liu, X. Deng, C. Ning, L. Zhou, L. Rong and B. Liu, *Biomater. Sci.*, 2019, **7**, 1995–2008.
14 E. Fu, K. Wallace, K. Grayden and M. Kaplan, *SN Compr. Clin. Med.*, 2021, **3**, 1586–1592.
15 H. Sabelström, M. Stenudd and J. Frisén, *Exp. Neurol.*, 2014, **260**, 44–49.
16 F. Barnabe-Heider, C. Goritz, H. Sabelstrom, H. Takebayashi, F. W. Pfrieger, K. Meletis and J. Frisen, *Cell Stem Cell*, 2010, **7**, 470–482.
17 A. J. Mothe and C. H. Tator, *Neuroscience*, 2005, **131**, 177–187.
18 X. Li, C. Fan, Z. Xiao, Y. Zhao, H. Zhang, J. Sun, Y. Zhuang, X. Wu, J. Shi, Y. Chen and J. Dai, *Biomaterials*, 2018, **183**, 114–127.
19 W. Xue, C. Fan, B. Chen, Y. Zhao, Z. Xiao and J. Dai, *Stem Cells*, 2021, **39**, 1025–1032.
20 S. Hu, Y. Chen, Z.-F. Wang, Q.-L. Mao-Ying, W.-L. Mi, J.-W. Jiang, G.-C. Wu and Y.-Q. Wang, *Evidence-Based Complementary Altern. Med.*, 2015, **2015**, 973524.
21 D.-d. Duan, K.-x. Wang, Y.-z. Zhou, X.-m. Qin, L. Gao and G.-h. Du, *Rejuvenation Res.*, 2017, **20**, 506–516.
22 K. v. Leyen, H. Y. Kim, S.-R. Lee, G. Jin, K. Arai and E. H. Lo, *Stroke*, 2006, **37**, 3014–3018, DOI: **https://doi.org/10.1161/01.STR.0000249004.25444.a5**.
23 Y. Chen, J. Zhang, M. Zhang, Y. Song, Y. Zhang, S. Fan, S. Ren, L. Fu, N. Zhang, H. Hui and X. Shen, *Clin. Transl. Med.*, 2021, **11**, e577.
24 F. Chen, M. Zhuang, C. Zhong, J. Peng, X. Wang, J. Li, Z. Chen and Y. Huang, *Oncol. Rep.*, 2015, **33**, 457–463.
25 R. Iwata and P. Vanderhaeghen, *Curr. Opin. Neurobiol.*, 2021, **69**, 231–240.
26 M. Agathocleous, N. K. Love, O. Randlett, J. J. Harris, J. Liu, A. J. Murray and W. A. Harris, *Nat. Cell Biol.*, 2012, **14**, 859–864.
27 X. Zheng, L. Boyer, M. Jin, J. Mertens, Y. Kim, L. Ma, L. Ma, M. Hamm, F. H. Gage and T. Hunter, *eLife*, 2016, **5**, e13374.
28 Y. Li, S. Lin, C. Xu, P. Zhang and X. Mei, *Biol. Pharm. Bull.*, 2018, **41**, 478–486.
29 C. Y. Wu, H. Xu, J. F. Li, X. L. Hu, X. Y. Wang, Y. J. Huang, Y. Li, S. R. Sheng, Y. L. Wang, H. Z. Xu, W. F. Ni and K. L. Zhou, *Front. Pharmacol.*, 2020, **11**, 12.
30 J. Zhang, Y. He, X. Jiang, H. Jiang and J. Shen, *Sci. China: Life Sci.*, 2019, **62**, 1332, DOI: **https://doi.org/10.1007/s11427-019-9587-y**.
31 H. Shen, C. Fan, Z. You, Z. Xiao, Y. Zhao and J. Dai, *Adv. Funct. Mater.*, 2022, **32**, 2110628.
32 S. Dinescu, M. A. Kaya, L. Chitoiu, S. Ignat, D. A. Kaya and M. Costache, *Cellulose-Based Superabsorbent Hydrogels* Polymers and Polymeric Composites: A Reference Series;, ed. M. Mondal, 2019, pp. 1-21.
33 L. Zhang, C. Fan, W. Hao, Y. Zhuang, X. Liu, Y. Zhao, B. Chen, Z. Xiao, Y. Chen and J. Dai, *Adv. Healthc. Mater.*, 2021, **10**, 2001896.
34 F. Tang, J. Tang, Y. Zhao, J. Zhang, Z. Xiao, B. Chen, G. Han, N. Yin, X. Jiang, C. Zhao, S. Cheng, Z. Wang,

Y. Chen, Q. Chen, K. Song, Z. Zhang, J. Niu, L. Wang, Q. Shi, L. Chen, H. Yang, S. Hou, S. Zhang and J. Dai, *Sci. China: Life Sci.*, 2022, **65**, 909–926.

35 Z. Xiao, F. Tang, J. Tang, H. Yang, Y. Zhao, B. Chen, S. Han, N. Wang, X. Li, S. Cheng, G. Han, C. Zhao, X. Yang, Y. Chen, Q. Shi, S. Hou, S. Zhang and J. Dai, *Sci. China: Life Sci.*, 2016, **59**, 647–655.

36 A. M. Gregus, S. Doolen, D. S. Dumlao, M. W. Buczynski, T. Takasusuki, B. L. Fitzsimmons, X.-Y. Hua, B. K. Taylor, E. A. Dennis and T. L. Yaksh, *Proc. Natl. Acad. Sci. U. S. A.*, 2012, **109**, 6721–6726.

37 C. Chen, J. Tang, Y. Gu, L. Liu, X. Liu, L. Deng, C. Martins, B. Sarmento, W. Cui and L. Chen, *Adv. Funct. Mater.*, 2019, **29**, 1806899.

38 C. M. Dumont, M. A. Carlson, M. K. Munsell, A. J. Ciciriello, K. Strnadova, J. Park, B. J. Cummings, A. J. Anderson and L. D. Shea, *Acta Biomater.*, 2019, **86**, 312–322.

39 X. Li and J. Dai, *Biomater. Sci.*, 2018, **6**, 265–271.

40 B. Chen, Z. F. Xiao, Y. N. Zhao and J. W. Dai, *Natl. Sci. Rev.*, 2017, **4**, 530–532.

41 B. Kaplan and S. Levenberg, *Int. J. Mol. Sci.*, 2022, **23**, 1244.

42 Z. Chen, H. Zhang, C. Fan, Y. Zhuang, W. Yang, Y. Chen, H. Shen, Z. Xiao, Y. Zhao, X. Li and J. Dai, *ACS Nano*, 2022, **16**, 1986–1998.

43 X. Li, Z. Xiao, J. Han, L. Chen, H. Xiao, F. Ma, X. Hou, X. Li, J. Sun, W. Ding, Y. Zhao, B. Chen and J. Dai, *Biomaterials*, 2013, **34**, 5107–5116.

44 C. Fan, X. Li, Y. Zhao, Z. Xiao, W. Xue, J. Sun, X. Li, Y. Zhuang, Y. Chen and J. Dai, *Biomater. Sci.*, 2018, **6**, 1723–1734.